J|A|C|S
COMMUNICATIONS

Growth of Long, Highly Stable, and Densely Packed Worm-Like Nanocolumns of Hexa-*peri*-Hexabenzocoronenes via Chemisorption on Au(111)

Luc Piot,[†] Camille Marie,[†] Xi Dou,[‡] Xinliang Feng,[‡] Klaus Müllen,*[,‡] and Denis Fichou*[,†]

CEA-Saclay, Labo Nanostructures et Semi-Conducteurs Organiques CNRS-CEA-UPMC, SPCSI, Bât. 462,
91191 Gif-sur-Yvette, France, Max-Planck-Institute for Polymer Research, Ackermanweg 10,
55128 Mainz, Germany

Received November 7, 2008; E-mail: denis.fichou@cea.fr

Since the discovery of discotic liquid crystals (DLCs) by Chandrasekhar et al. in 1977,[1] a wealth of disk-shaped aromatic cores surrounded by peripheral flexible chains have been synthetized.[2] DLCs self-assemble into columnar mesophases as a result of strong $\pi-\pi$ interactions between aromatic cores and possess 1D charge transport properties which make them attractive for applications such as xerography, solar cells, and field-effect transistors.[3,4] Although DLC stacks can be oriented vertically on a substrate, a number of processing techniques have been developed to produce horizontal columnar order with an edge-on arrangement of the molecules. This is particularly the case for hexa-*peri*-hexabenzocoronenes (HBCs), one prominent class of DLCs with high supramolecular order and anisotropic charge carrier mobilities. Zone casting[5] and mechanical[6] or electrical[7] alignment are a few examples of techniques which have been utilized to produce planar alignment of HBC columnar layers.

Along this line, we recently reported on the hierarchical self-assembly of hexakis-(*n*-dodecyl)-*peri*-hexabenzocoronene (HBC-C_{12}) into extended uniaxial columnar stacks growing spontaneously at a liquid/solid interface.[8] Scanning tunneling microscopy (STM) reveals that these nanocolumns physisorb on highly oriented pyrolitic graphite (HOPG) and form multilayered superstructures of the type {HOPG/face-on/edge-on/edge-on} and {HOPG/face-on/edge-on/face-on}. STM images with molecular resolution provide direct insight into the inter- and intracolumnar morphology. However, physisorption of HBCs nanocolumns does not ensure long-term stability because of too weak interactions with the substrate and therefore is not appropriate for device applications.

To produce planar alignments of HBCs nanocolumns having good resistance against mechanical or electrical constraints, it is necessary to graft them chemically on the substrate. We also expect chemisorption to produce more densely packed nanocolumns (as compared to physisorption) because of the larger number of potential adsorption sites on the substrate. A widespread method to form molecular self-assembled monolayers (SAMs) is to take advantage of the ability of the sulfur atom to link covalently on various metals.[9,10] The challenge is then to combine chemisorption together with planar columnar alignment via $\pi-\pi$ interaction between the HBC cores.

We report here on the growth of persistent edge-on HBC nanocolumns chemically grafted on gold via terminal anchoring groups containing sulfur atoms. The two HBC derivatives that we designed to this purpose bear five 3,7-dimethyloctyl solubilizing groups, the sixth peripheral substituent being terminated by either a thioacetate group (HBC-Sac) or a 1,2-dithiolate ring (HBC-SS) (Figure 1). It has already been reported that these two groups lead to the formation of SAMs on gold.[11] Also, the side-chain bearing the thioacetate function of the HBC-Sac molecule is rather short (~10.3 Å) and rigid whereas the chain bearing the disulfur group of HBC-SS is long (~18.6 Å) and flexible. By tuning the length and flexibility of the grafting chain we expect to influence the $\pi-\pi$ stacking of the HBC cores and hence the length and conformation of the columns.

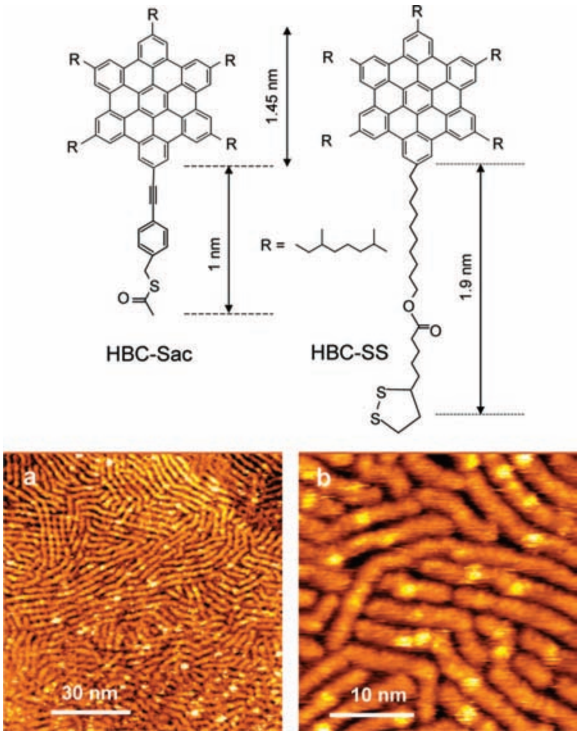

Figure 1. Top: Chemical structures of HBC-Sac and HBC-SS. Bottom: STM images of HBC-Sac nanocolumns chemisorbed on Au(111) after deprotection of the thioacetate terminal group. (a) 104.5 × 104.5 nm^2; I_t = 77 pA; V_t = 1.35 V. (b) 31 × 31 nm^2; I_t = 30 pA; V_t = 1.30 V.

The synthesis of HBC-SS has been described elsewhere,[12] while that of HBC-Sac is described in the Supporting Information, SI. Prior to adsorption on gold, the protecting acetate function of HBC-Sac is removed by reaction with NH_4OH in an EtOH/THF (1:2) mixture. HBC edge-on nanocolumns are prepared by immersing for 20 min a flame-annealed reconstructed Au(111) substrate (Goodfellow, 150 nm deposited on mica) in a solution of the appropriate molecule (5 × 10^{-7} mol·L^{-1}) in *n*-tetradecane (Aldrich, 99.9%). After removal of the gold substrate from the solution, the samples are rinsed by *n*-tetradecane to remove nonadsorbed molecules and dried in a stream of dry nitrogen. A droplet of fresh *n*-tetradecane is then deposited on the sample for STM observation

---

[†] CEA-Saclay.
[‡] Max-Planck-Institute for Polymer Research.

10.1021/ja808752b CCC: $40.75 © 2009 American Chemical Society

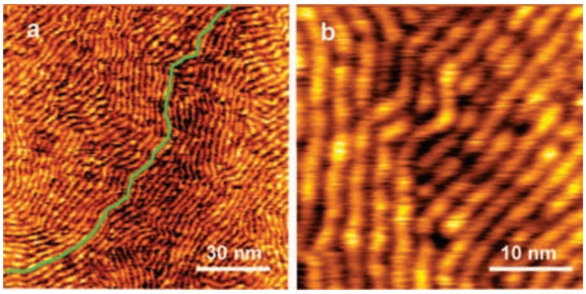

Figure 2. STM images of HBC-SS nanocolumns chemisorbed on Au(111). (a) 115 × 115 nm^2; I_t = 11 pA; V_t = 2 V. The green line materializes in uninterrupted nanocolumns ~130 nm in length. (b) 32.4 × 32.4 nm^2; I_t = 14 pA; V_t = 2 V.

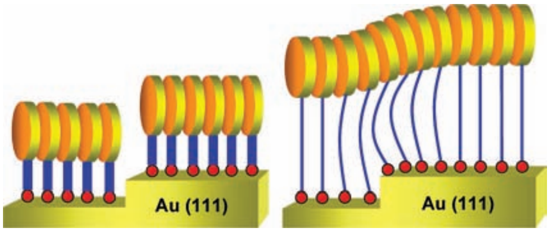

Figure 3. Schematic structure of HBC nanocolumns chemisorbed on Au(111) via sulfur atoms (as red circles) showing the "disruptive" step crossing of HBC-Sac bearing a short and rigid grafting chain (left) and the "soft" step crossing of HBC-SS bearing a long and flexible chain (right). Note that the vertical orientation of the HBC molecules is arbitrary and does not reflect any experimental evidence.

at the liquid/solid interface[13−17] in constant-current mode at room temperature using a Pico-SPM (Molecular Imaging/Agilent Technology).

The STM image of Figure 1a shows that deprotected HBC-Sac chemisorbs on gold by forming a densely packed monolayer of nanocolumns with a surface coverage close to 100%. No change is observed on the STM images after rinsing the samples with various organic solvents (ethanol, acetone, etc.), exposure to air or vacuum, or several days left in open air, thus indicating their high stability and strong attachment on gold. Individual columns have a worm-like conformation with no preferential direction but associate parallel to each other into small groups. Their length (see histogram in SI) varies from 3 to 70 nm, with 85% of the columns being concentrated in the narrow 3−30 nm range. The in-plane intercolumnar spacing is ~2.8 nm as determined by an STM cross-section (see SI). The latter value is similar to the intercolumnar distance of HBC-C_{12} measured by X-ray diffraction but considerably smaller than that of nanocolumns physisorbed at the graphite/*n*-tetradecane interface (~4.8 nm).[8] Higher resolution (Figure 1b) shows that a number of nanocolumns are bent into two segments making an angle > 90°. Such a shape reveals intracolumnar defects in the $\pi-\pi$ stacking whose origin is probably governed by the nature and number of the potential adsorption sites of gold. Unfortunately, since the Au(111) surface is no longer visible after adsorption of the HBC-Sac columns, it is difficult to confirm by STM and more surface characterizations are needed and presently under way.

In an attempt to increase the length and orientation of the nanocolumns, we increased the length and flexibility of the spacer bearing the grafting function. In Figure 2, HBC-SS adsorbs on gold into nanocolumns whose length varies from 30 to 210 nm (see histogram in SI), with only 70% of the columns in the wide 30−10 nm range. The HBC-SS nanocolumns possess the same stability properties as the HBC-Sac ones. Although nonlinear, they are parallel to each other and oriented in preferential directions in a brushing manner. The intercolumnar spacing between consecutive and parallel columns is again ~2.8 nm, identical to that for HBC-Sac. The higher ordering degree of HBC-SS columns as compared to HBC-Sac confirms that long and flexible spacers favor the $\pi-\pi$ stacking of the HBC cores.

A feature directly related to the length and flexibility of the grafting leg is observed at the gold step edges. While most of HBC-Sac columns are interrupted by the monatomic gold steps (height = 2.4 Å) because of a short and rigid grafting leg, the HBC-SS ones easily cross them without interruption due to a longer and more flexible spacer (Figures S3,S4 in SI). This is illustrated in Figure 3 where the spacers are marked in thick (HBC-Sac) and thin (HBC-SS) blue lines. We anticipate that shorter nanocolumns together with a disruptive crossing of the gold steps will strongly affect charge transport along the columns thus resulting in lower carrier mobilities.

We demonstrate here for the first time that highly stable and densely packed edge-on nanocolumns of HBCs spontaneously grow from solution as self-assembled monolayers chemisorbed on gold. Their degree of ordering and length, and hence their transport properties, are directly related to the length and flexibility of the spacer bearing the grafting chemical function. We now study the growth of HBC edge-on nanocolumns on various insulating substrates and envisage them as the active layer in devices such as field-effect transistors.

Supporting Information Available: Additional experimental details. This material is available free of charge via the Internet at http://pubs.acs.org.

References

(1) Chandrasekhar, S.; Sadashiva, B. K.; Suresh, K. A. *Pramana* **1977**, *9*, 471.
(2) Kumar, S. *Chem. Soc. Rev.* **2006**, *35*, 83.
(3) Schmidt-Mende, L.; Fechtenkötter, A.; Müllen, K.; Moons, E.; Friend, R. H.; MacKenzie, J. D. *Science* **2001**, *293*, 1119.
(4) Laschat, S.; Baro, A.; Steinke, N.; Giesselmann, F.; Hägele, C.; Scalia, G.; Judele, R.; Kapatsina, E.; Sauer, S.; Schreivogel, A.; Tosoni, M. *Angew. Chem., Int. Ed.* **2007**, *46*, 4832.
(5) Piris, J.; Debije, M. G.; Stutzmann, N.; Laursen, B. W.; Pisula, W.; Watson, M. D.; Bjornholm, T.; Müllen, K.; Warman, J. M. *Adv. Funct. Mater.* **2004**, *14*, 1053.
(6) Van de Craats, A. M.; Stutzmann, N.; Bunk, O.; Nielsen, M. M.; Watson, M. D.; Müllen, K.; Chanzy, H. D.; Sirringhaus, H.; Friend, R. H. *Adv. Mater.* **2003**, *15*, 495.
(7) Cristadoro, A.; Lieser, G.; Räder, H. J.; Müllen, K. *ChemPhysChem.* **2007**, *8*, 586.
(8) Piot, L.; Marie, C.; Feng, X.; Müllen, K.; Fichou, D. *Adv. Mater.* **2008**, *20*, 3854.
(9) Love, J. C.; Estroff, L. A.; Kriebel, J. K.; Nuzzo, R. G.; Whitesides, G. M. *Chem. Rev.* **2005**, *105*, 1103.
(10) Jiang, P.; Nion, A.; Marchenko, A.; Piot, L.; Fichou, D. *J. Am. Chem. Soc.* **2006**, *128*, 12390.
(11) Tour, J. M.; Jones, L., II; Pearson, D. L.; Lamba, J. J. S.; Burgin, T. P.; Whitesides, G. M.; Allara, D. L.; Parikh, A. N.; Atre, S. *J. Am. Chem. Soc.* **1995**, *117*, 9529.
(12) Duati, M.; Grave, C.; Tcbeborateva, N.; Wu, J. S.; Müllen, K.; Shaporenko, A.; Zharnikov, M.; Kriebel, J. K.; Whitesides, G. M.; Rampi, M. A. *Adv. Mater.* **2006**, *18*, 329.
(13) De Feyter, S.; De Schryver, F. C. *Chem. Soc. Rev.* **2003**, *32*, 139.
(14) Mena-Osteritz, E.; Bauerle, P. *Adv. Mater.* **2001**, *13*, 243.
(15) Katsonis, N.; Marchenko, A.; Fichou, D. *J. Am. Chem. Soc.* **2003**, *125*, 13682.
(16) Samori, P.; Müllen, K.; Rabe, J. P. *Adv. Mater.* **2004**, *16*, 1761.
(17) Piot, L.; Marchenko, A.; Wu, J. S.; Müllen, K.; Fichou, D. *J. Am. Chem. Soc.* **2005**, *127*, 16245.

JA808752B